applied sciences

MDPI

Communication

The Use of Copper Slag in the Thermolysis Process for Solar Hydrogen Production—A Novel Alternative for the Circular Economy

Manuel Fuentes [1,2,*], Susana Leiva-Guajardo [1], Atul Sagade [2], Felipe Sepúlveda [1], Alvaro Soliz [3], Norman Toro [4], José Ángel Cobos Murcia [5], V. E. Reyes Cruz [5], Mario Toledo [6], Edward Fuentealba [1] and Felipe M. Galleguillos Madrid [1,*]

1 Centro de Desarrollo Energético Antofagasta, Universidad de Antofagasta, Antofagasta 1240000, Chile; susana.leiva.guajardo@ua.cl (S.L.-G.); felipe.sepulveda@uantof.cl (F.S.); edward.fuentealba@uantof.cl (E.F.)
2 Departamento de Ingeniería Mecánica, Universidad de Tarapacá, Arica 1100000, Chile; asagade@academicos.uta.cl
3 Departamento de Ingeniería en Metalurgia, Universidad de Atacama, Copiapó 1531772, Chile; alvaro.soliz@uda.cl
4 Facultad de Ingeniería y Arquitectura, Universidad Arturo Prat, Iquique 1110939, Chile; notoro@unap.cl
5 Instituto de Ciencias Básicas e Ingeniería, Universidad Autónoma del Estado de Hidalgo, Carr. Pachuca—Tulancingo km. 4.5, Mineral de la Reforma 42184, Mexico; jose_cobos@uaeh.edu.mx (J.Á.C.M.); profe_4948@uaeh.edu.mx (V.E.R.C.)
6 Department of Mechanical Engineering, Universidad Técnica Federico Santa María, Av. España 1680, Valparaíso 2390123, Chile; mario.toledo@usm.cl
* Correspondence: msfuentes@academicos.uta.cl (M.F.); felipe.galleguillos.madrid@uantof.cl (F.M.G.M.); Tel.: +56-9-4526-5145 (M.F.); +56-9-4235-2163 (F.M.G.M.)

Abstract: Copper slag, produced in pyrometallurgical processes, has the potential to generate hydrogen through thermolysis, depending on its composition. This manuscript explores the use of copper slag as a highly abundant and low-cost material for thermochemical water splitting using concentrated solar power. Copper slag can undergo endothermic reactions with water vapor at high temperatures, conditions which are favorable for activating hydrogen evolution reactions which can be a potential resource for metal recovery such as magnetite and hematite in the circular economy. While research on copper slag and its components has primarily focused on the recovery of valuable metals and material reuse, its direct application in hydrogen production remains largely unexplored, partly due to historically low interest in hydrogen as an energy source. The vast deposits of copper slag in the Atacama Desert, combined with the growing demand for renewable energy, present a unique opportunity to develop sustainable and cost-effective hydrogen production technologies.

Keywords: circular economy; copper slag; waste management; water splitting at high temperature

check for updates

Academic Editor: Davide Mombelli

Received: 13 March 2025
Revised: 8 April 2025
Accepted: 10 April 2025
Published: 30 April 2025

Citation: Fuentes, M.; Leiva-Guajardo, S.; Sagade, A.; Sepúlveda, F.; Soliz, A.; Toro, N.; Cobos Murcia, J.Á.; Reyes Cruz, V.E.; Toledo, M.; Fuentealba, E.; et al. The Use of Copper Slag in the Thermolysis Process for Solar Hydrogen Production—A Novel Alternative for the Circular Economy. *Appl. Sci.* **2025**, *15*, 4988. https://doi.org/10.3390/app15094988

Copyright: © 2025 by the authors. Licensee MDPI, Basel, Switzerland. This article is an open access article distributed under the terms and conditions of the Creative Commons Attribution (CC BY) license (https://creativecommons.org/licenses/by/4.0/).

1. Introduction

From an extensive review of the literature, it has been seen that the use of copper slag is not yet considered to be alternative for the cathode materials that currently exist in the thermolysis processes used in the production of solar hydrogen. Copper slag, due to its physical and mechanical characteristics, can be used to manufacture products such as cement, filler, railway ballast, abrasives, aggregates, roofing granules, glass, tiles, etc. In addition, valuable metals can be recovered through various extractive metallurgical routes, such as reduction by direct high-temperature smelting [1]. Shot-peened copper slag has

also been used as a fine aggregate in Portland cement concrete. Wang et al. [2], indicate that the most common management for copper slag is recycling to produce value-added products, such as abrasive tools, and granule cutting tools for roofing, tiles, and road base construction [2–5]. Research related to copper slag is aimed at finding reuse applications for it as a construction material [3], using high-temperature, direct reduction in slag as a means of waste management [6], as a material for the manufacture of high-strength concrete [7], as a potential catalyst (iron present in the slag) for the depletion of phenol present in water during hydrogen peroxide (H_2O_2) production [8], in the recovery of valuable metals from slag [9–11], in the recovery of iron from copper slag by direct reduction based on coal [1], as a bifunctional photocatalyst for the degradation of alcohols and hydrogen production [12,13], in thermal energy storage systems [14,15], and in the recovery of copper and magnetite from copper slag using concentrated solar power (CSP) [16].

Among the research carried out with copper slag, its main use has focused on the recovery of valuable metals such as Co and Cu. Currently, solar thermochemical cycles are based on the use of materials from rare earths such as cerium oxide (CeO_2), which is insufficient and expensive [17,18]. However, there is no evidence in the scientific literature of the direct use of copper slag as a thermo-catalytic material for the generation of gaseous hydrogen through a solar thermochemical process. In addition to the above, the abundance of copper slag in the Atacama Desert, mainly that deposited in abandoned landfills, generates one of the largest environmental liabilities related to the processes of obtaining copper [19], which to date has no solution [20].

The smelting of copper concentrate (20–30% Cu) composed of bornite (Cu_5FeS_4), chalcopyrite ($CuFeS_4$), pyrite (FeS_2), covellite (CuS) and chalcocite (Cu_2S) [21,22], enters the smelting furnace at temperatures of 1200–1300 °C, releasing gases such as O_2, SO_2, N_2, CO, CO_2, and H_2 due to the compositions of the fluxes used such as natural gas, thermal coal, and metallurgical coke [23], with the resultant (Matte) containing a Cu content between 35 and 75%. The copper slag generated normally contains FeO, Fe_3O_4, SiO_2, Al_2O_3, MgO, CaO, and Cu_2O [24]. Phiri et al. have investigated in-depth the presence of TiO_2, MnO, As, Pb, and other chemical elements [25], which makes it a complex multi-component residual material. However, it is mainly composed of Fe (40 wt%), Si (15–37 wt%), and Cu (0.8–13 wt%) [21].

This communication highlights the importance of copper slag in the thermolysis process for H_2 production, examining its role in the circular economy and the potential benefits of treating slag waste through thermochemical methods. By integrating copper slag into solar-driven thermolysis, it is possible to add economic value to existing applications—improving energy efficiency, enabling hydrogen generation, and recovering valuable metals such as Fe_3O_4 y Fe_2O_3. This approach helps reduce the environmental impact of Cu production by transforming industrial waste into a useful raw material.

2. Production of Copper Slag

The smelting process involves separating Cu, the primary element, from contaminants or impurities that diminish its economic value, to obtain a high degree of purity. The copper smelting process typically comprises five main stages: (i) flotation, (ii) smelting, (iii) conversion, (iv) fire refining, and (v) electrolytic refining [26]. Figure 1 shows the process in which, during the smelting stage, the copper concentrate (20–30% Cu), composed of Cu_5FeS_4, $CuFeS_2$, FeS_2, and Cu_2S, enters the smelting furnace at approximately 1200 °C, releasing gases such as O_2, SO_2, N_2, CO, CO_2, H_2, and H_2O (v). The resulting slag and matte (Cu_2S and FeS) contain between 35 and 75% Cu. During the conversion stage, sulfur and iron present in the sulfide phase are removed through an oxidation process, yielding relatively pure Cu metal, known as blister Cu (approximately 99% Cu). At this stage,

copper slag is formed, primarily composed of FeO, Si, and $CaCO_3$, resulting in a slag with low Cu content. In the refining stage, the blister copper still contains impurities such as Ag, Au, As, Sb, Bi, and Fe. The final stage, electrorefining, is used to recover Cu with a purity of 99.9% from the initial concentrate (20–30% Cu). Copper slag typically contains components such as FeO, Fe_3O_4, SiO_2, Al_2O_3, MgO, CaO, and Cu_2O [21].

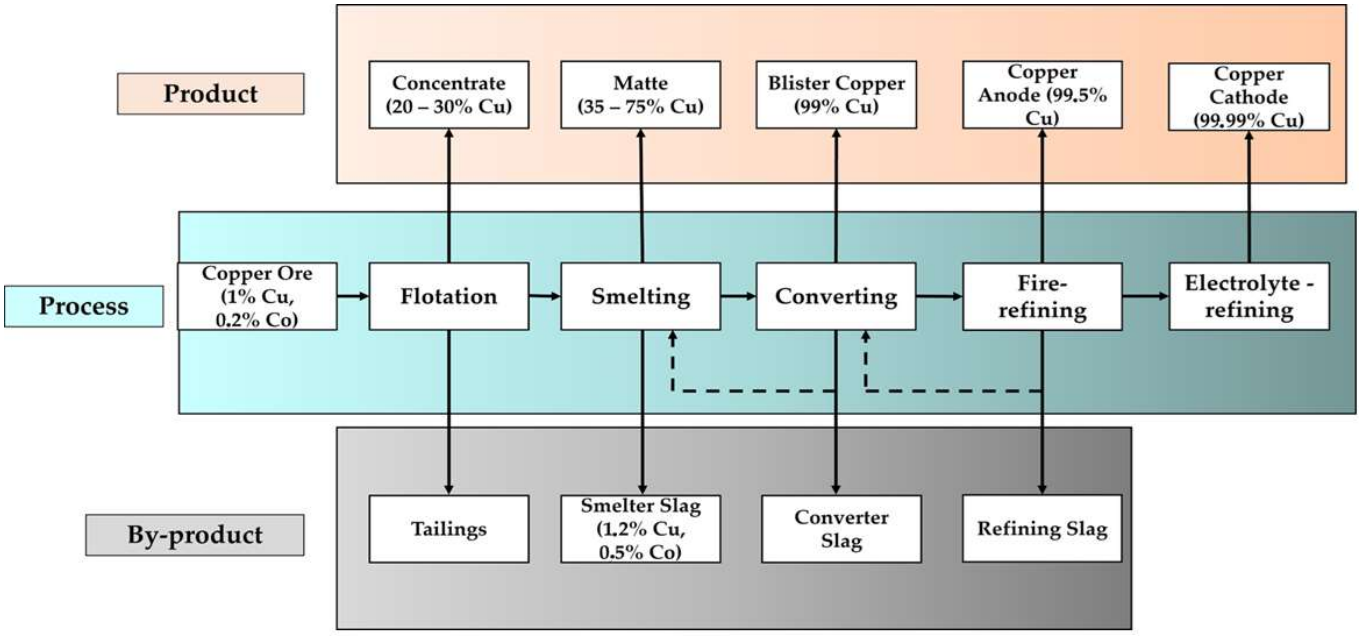


Figure 1. Scheme of Cu slag production, process, product, and by-product (modified of [21]).

Copper Slag

Copper slag is a by-product generated during the pyrometallurgical process used to extract concentrated copper from sulfide mineral ores. It typically contains materials such as FeO, SiO_2, Al_2O_3, CaO, and residual Cu [3]. The pyrometallurgical stage, known as smelting, involves the use of furnaces operating at very-high temperatures. During this process, the intense heat generates two immiscible liquid phases: a Cu-rich matte and a copper slag referred to as the oxide phase [19]. Generally, copper slag is composed of oxides such as FeO and Fe_3O_4 (30–40%), SiO_2 (35–40%), Al_2O_3 (0–10%), and CaO (0–10%) [3] which vary their presence in the product slag due to (i) the nature of the minerals, (ii) the nature of the fluxes, (iii) the nature of the concentrates, and (iv) the operating conditions, as well as other factors related to the production process [27]. Copper slag is one of the main solid wastes from the pyrometallurgical process that is applied to concentrates in copper industry plants. Chile produces approximately 4.5 million tons of slag per year, and more than 30 million tons of copper slag are produced annually in the world [28], demonstrating the magnitude of the waste from mining mineral processing. Furthermore, copper slag often contains a large amount of valuable metal and is currently considered a secondary metal resource [6]. These metals can be Fe, Cr, Cu, Al, Zn, Co, Ni, Nb, Ta, Au, and Ag, and they can be recovered by units operated in the mineral processing of slags, such as (i) crushing, (ii) grinding, (iii) magnetic separation, (iv) flotation, (v) leaching, and (vi) roasting [9], respectively. Materials used for cathodes have become increasingly important [29]. Therefore, recycling the metals present in copper slag can not only recover strategic metals but also contribute to carbon neutrality. Regarding their appearance and properties, naturally cooled copper slags have a black color and a glassy surface, and are dense, lumpy, hard, and brittle (see Table 1). Important properties to consider for use in a thermochemical solar process are the unit weight (transport), bulk density

(storage), and hardness (abrasive material). However, depending on the cooling pattern, which can be natural or water quenched, they can differ in appearance, density, and shape (see Table 2) [30].

Table 1. Physical and mechanical properties of copper slag [3,31].

Property	Value
Unit weight (T/m^3)	2.8–3.8
Absorption	0.13
Bulk density (T/m^3)	2.3–2.6
Conductivity (µs/cm)	500
Specific gravity	2.8–3.8
Hardness (Moh)	6–7
Moisture (ppm)	<5
Abrasion loss (%)	2.4–10
Internal friction angle	40–53

Table 2. Visual description of copper smelting slag.

Property	Description	Ref.
Particle shape	Angular	[32–34]
	Irregular	[31,35,36]
	Multifaceted	[37]
Surface texture	Glassy	[24,32,34,36]
	Smooth	[6,9,31,33,38,39]
	Granular rough	[34,40,41]
Color	Black	[32,42]
	Blackish gray	[43,44]
	Brown with green, red, or black tint	[45]

In recent years (1999–2019), approximately 752 Mt [20] of copper smelting slag have been generated from the 13 main producing countries (see Figure 2). The largest generation of this waste occurs in South America (40%), followed by Asia (13%), USA (8%), Oceania (6%), Europe (6%), Africa (6%), and others (15%).

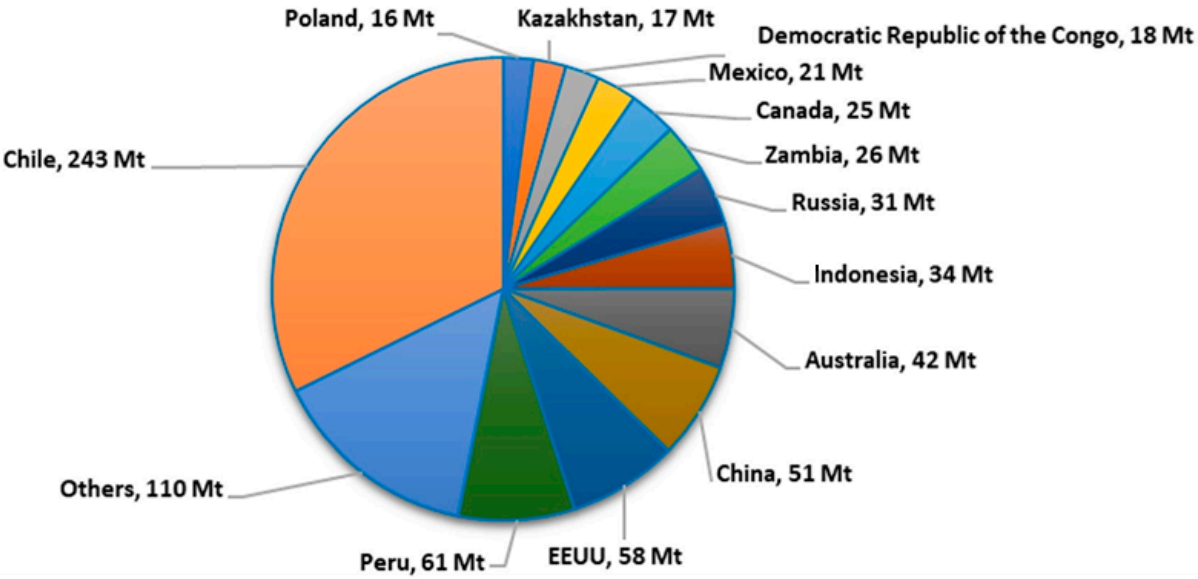


Figure 2. Copper slag was generated worldwide between 1999 and 2019 (adapted from [20]).

In Chile there are seven copper smelters, five of them are state-owned and the other two are private. The location, capacity, and production of the Chilean smelters are reported in Figure 3. Among the state-owned smelters, four are under the jurisdiction of the National Copper Corporation (CODELCO), Chuquicamata (Calama), Potrerillos (El Salvador), Ventanas (Puchuncaví), and Caletones (Rancagua), with a smelting capacity of 3880 kt/y (63.08% national capacity), while one operates under the National Mining Company (ENAMI) with a capacity of 450 kt/y (7.33% national capacity), which is the Hernan Videla Lira Smelter Plant (Copiapó). The remaining two smelters, Alto Norte (Xstrata, Antofagasta) and Chagres (Anglo American, Catemu), are privately owned [46]. At Caletones, Potrerillos, and Chuquicamata, they are transitioning from slag treatment furnaces to grinding and flotation processes. It is noteworthy to emphasize that between 1999 and 2019, Chile has accounted for approximately one-third of global copper smelting slag production. This equates to an average annual output of 12 million tons, stemming from the seven copper smelters within the country [6].

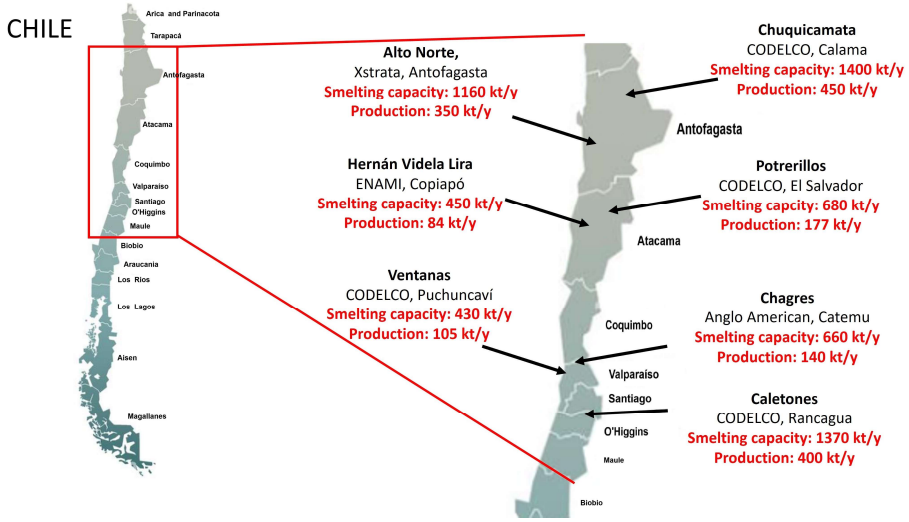


Figure 3. Location, capacity, and production of the Chilean smelters.

3. Discussion

Copper slag is a massive by-product of the mining industry, generated in large volumes annually worldwide. Traditionally considered a waste material, its composition rich in metal oxides makes it attractive for advanced applications, such as its use as a cathodic electrode to promote hydrogen evolution reactions (HERs) during the thermochemical cathodic subprocess. Its implementation as a cathode material for H_2 production represents a disruptive innovation for several reasons: (i) instead of being discarded or underutilized, copper slag can be treated and transformed into functional electrodes, extending its life cycle and reducing the need to extract new resources—thus closing the material use loop, a core principle of the circular economy; (ii) the presence of iron oxides and iron silicate (Fe_2SiO_4) gives the slag a porous structure and sufficient conductivity to act as a redox-supporting conductor in systems for water treatment, due to its tendency to produce H_2O_2, or in alkaline electrolysis for HERs; (iii) reusing copper slag as an electrode prevents its disposal in legal or illegal landfills, reducing the occupation of large volumes of public land. Moreover, by replacing exotic materials like Ti, Pt, or Ni, it reduces reliance on costly and uncommon metals, and lowers the carbon footprint and energy consumption in the fabrication of electrochemical devices; (iv) manufacturing electrodes from copper slag allows a significant reduction in costs, which is crucial in efforts to democratize technologies such as wastewater treatment or distributed hydrogen generation [2–5].

The elemental characterization of copper slag in Chile has been extensively reported by Nazer et al. [21,24], and the researchers indicate that modern copper slags possess high contents of SiO_2 (10–71%) and FeO (0.7–62%) and the predominant chemical elements correspond to Cu, Pb, Ni, and Zn, with its mineralogical phases being mainly Fe_2SiO_4 and Fe_3O_4 [24,47,48]. The variation in the elemental and mineralogical chemical composition of copper slag is mainly influenced by the type of (i) concentrate, (ii) type of fluxes, (iii) type of furnace, and (iv) cooling rates during and after the smelting and converting processes [25]. Table 3 shows the different compositions of copper slag provided through the scientific literature, in which the high contents of Fe, Fe_2O_3, FeO, and SiO_2 stand out. However, the extensive scientific literature indicates that compounds containing Fe, FeO, Fe_2O_3, and Fe_3O_4 react with water steam at high temperatures to generate H_2 gas [49]. It is reported that at 900 °C, 1.43 mol H_2/kg was produced from high-temperature steam steel slag [50,51]. Nevertheless, the mineralogical study in Chile of the copper slag indicates that it is composed of 50% Fe_2SiO_4, 39% Fe_3O_4, and 10% $(Mg,Fe)_2SiO_4$ [7]. There is then the possibility that copper slag deposited in Chile reacts with water steam to generate H_2 because its main compounds contain iron oxides.

The XRD analysis of the copper slag from the Chilean smelter indicates that it is composed of, Fe_2SiO_4, Fe_3O_4, $KAl_2[AlSi_3O_{10}](OH)_2$, $Cu_6Si_2S_7$, $(Mg,Fe)_2SiO_4$, and $Ca_2Mg_5Si_8O_{22}(OH)_2$, show-up in the Figure 4a. Apart from the X-ray diffraction (XRD) and scanning electron microscopy with energy dispersive spectroscopy (SEM-EDS) examination shown in Figure 4, the findings in Figure 5 provide additional support for the chemical and mineralogical description of copper slag from Chile. Fe, Si, and O are the most common components in the sample, as shown by the SEM-EDS image. This is in line with the majority composition of Fe_2SiO_4 found in the earlier investigation.

Additionally, a spatial depiction of the primary components is provided by the elemental mapping). The micrographs' high concentrations of Fe, Si, and O support the idea that Fe_2SiO_4 is the predominant mineralogical phase. In accordance with the compounds found in the XRD analysis (Figure 4a), such as $Cu_6Si_2S_7$, trace amounts of Cu are also detected, indicating the potential presence of copper sulfides or silicates in the sample. When these methods are combined, it is confirmed that the examined slag retains a composition rich in Si and Fe, mostly in the form of Fe_3O_4 and Fe_2SiO_4, with $(Mg,Fe)_2SiO_4$ and $KAl_2[AlSi_3O_{10}](OH)_2$ as secondary minerals. This information is essential for evaluating the slags possible industrial uses and value as well as its reactivity in particular environmental settings.

The oxidation of a metal or metal oxide at high temperature is influenced by (i) the temperature, (ii) the composition of the gases generated, (iii) the time of exposure to the corrosive environment, and (iv) the pressure of the system, and is characterized by the reduction in the thickness (penetration) of the metal and the rate of formation of corrosion products. The oxidation rate increases significantly with increasing temperature [52], creating a homogeneous medium and improving the thermodynamic equilibrium [53]. When a metal is exposed to oxidation at high temperatures (corroded metal or thermal degradation), considering the reaction $xM + yH_2O \rightarrow MxOy + yH_2$ [52], a value of the Gibbs free energy (activation energy) is obtained, as determined by Equations (1) and (2):

$$\Delta G^{\circ} = -RT \ln(K) \quad (1)$$

$$\Delta G^{\circ} = -yRT \ln(PH_2/PH_2O) \quad (2)$$

During the oxidation process of a metal (M) exposed to water vapor, H_2 can be produced by the following reaction [54]:

$$MO_{(x-1)} + H_2O \rightarrow MO_x + H_2 \quad (3)$$

where the expression for the Gibbs free energy is as follows:

$$\Delta G^{\circ} = \Delta H^{MO_x} - \Delta H^{MO_{(x-1)}} - \Delta H^{H_2O} - T(S^{H_2} - S^{H_2O}) \leq 0 \quad (4)$$

where MO_x is the oxidized metal and MO_{x-1} is the reduced oxide, respectively.

The gas data published by Johansen et al. in 1970 [55] regarding the behavior of copper in the direct smelting process at 1300 °C considers among its analyses materials such as iron silicate and magnetite. However, specific thermodynamic data for copper slag have been presented in studies focused on metal recovery using the direct reduction smelting method [1]. The lack of information regarding thermodynamic data related to the oxidation of copper slag in water vapor and at high temperatures provides an interesting line of research that would significantly contribute to generating valuable information regarding the reduction in mining pollutants resulting from the use of slag in electrochemical processes, providing unprecedented added value. However, it is known that the generated copper slag normally contains metal oxides (FeO, Fe_3O_4, SiO_2, Al_2O_3, MgO, CaO, and Cu_2O), with its mineralogical phases being mainly Fe_2SiO_4 and Fe_3O_4 [24].

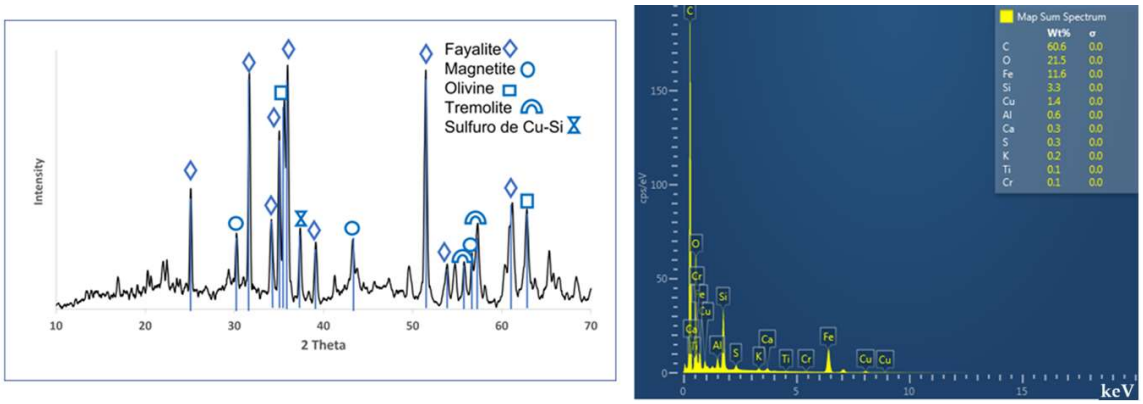


Figure 4. XRD analysis and EDX analysis of Chilean copper slag.

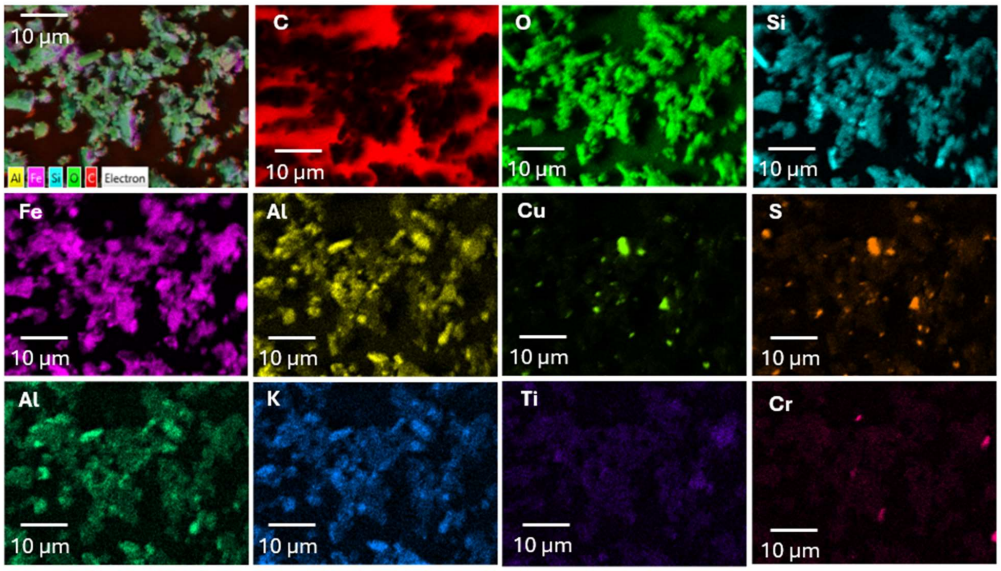


Figure 5. SEM-EDS indicates that the elements with the greatest presence are Fe, Si, O, and other primary components.

Table 3. Composition of the different copper slags published in scientific journals.

Country	Company	Cu	Fe	S	K	P	Fe_2O_3	FeO	SiO_2	CaO	Al_2O_3	MgO	P_2O_5	SO_3	CuO	K_2O	Na_2O	MnO	TiO_2	Ref.
Chile	O'Higgins. El Teniente.Converter, Rancagua	4.56	40.30	1.53	0.80	-	-	-	20.30	0.33	2.86	0.75	-	-	-	-	1.20	-	-	[21]
Chile	O'Higgins.El Teniente. Reververo furnace, Rancagua	0.83	33.30	0.50	1.10	-	-	-	37.90	7.70	7.50	1.40	-	-	-	-	2.10	-	-	[21]
Chile	Atacama, Century scoriales XIX Playa Negra, Copiapo	-	-	-	-	-	14.23	18.99	35.00	17.05	6.69	1.41	0.49	0.40	0.77	1.21	0.81	0.17	0.27	[19]
Chile	Atacama, Century scoriales XIX Canto del Agua, Copiapo	-	-	-	-	-	12.87	29.60	39.39	4.32	4.62	1.30	0.75	1.14	1.40	0.32	0.33	0.05	0.14	[19]
Chile	Atacama, Century scoriales XIX Nantoco, Copiapo	-	-	-	-	-	13.58	22.71	38.58	7.66	6.57	1.13	0.70	0.53	1.83	1.01	0.58	0.30	0.13	[19]
China	Tongling Non-ferrous Metals Group Holding Co., Ltd., Tongling, Anhui	0.80	39.10	0.45	-	0.10	-	42.85	31.11	2.44	2.29	1.79	-	-	-	-	-	-	-	[56]
Spain	Cabezo Juré archeological settlement, Alosno, Provincia de Huelva.	20.1	-	-	-	-	50.60	-	13.81	0.20	1.79	0.20	0.058	-	-	0.01	0.26	-	0.307	[57]
Mexico	Company and location unknown	-	-	-	-	-	45.46	-	33.12	11.68	4.67	0.42	0.10	-	-	0.77	2.64	0.39	0.22	[58]
Mexico	Smelter of the Mining-Metallurgical Complex of La Caridad, Sonora	1.05	44.57	-	-	-	-	-	25.12	-	-	-	9.42	-	-	-	-	-	-	[59]
Mexico	Industrias Magnelec SA de CV, Saltillo, Coah	-	-	-	-	-	0.13	-	0.2	1.00	0.15	98.5	-	-	-	-	-	-	-	[60]

Table 3. *Cont.*

Country	Company	Cu	Fe	S	K	P	Fe_2O_3	FeO	SiO_2	CaO	Al_2O_3	MgO	P_2O_5	SO_3	CuO	K_2O	Na_2O	MnO	TiO_2	Ref.
Italy	Campigilia Marittima Century scoriales XI-XIII. Capattoli	-	-	-	-	-	-	42.53	20.06	8.26	2.93	0.72	-	-	-	0.74	0.02	-	-	[61]
Italy	Campigilia Marittima Century scoriales XI-XIII. Capattoli	-	-	-	-	-	-	52.17	30.60	15.62	5.06	0.90	-	-	-	1.20	0.07	-	-	[61]
Portugal	District Sao Domingos Mining Centre, Century XX, Moitinha, Achada do Gamo	-	-	-	-	-	52.86	-	37.70	1.14	3.93	0.40	0.20	-	-	1.04	0.25	0.07	0.688	[62, 63]
Namibia	Dundee Precious Metals Ltd., Tsumeb smelting complex, Windhoek	-	-	6.51	-	-	32.47	9.49	14.68	4.50	4.70	1.43	0.59	-	-	0.30	0.26	0.08	0.25	[64, 65]
India	Sterlite Industries India Limited, Tuticorin, Tamil Nadu	-	-	-	-	-	61.24	-	19.72	5.65	3.03	0.90	0.63	3.31	1.49	1.23	-	0.08	0.44	[10]
Australia	Tropical coastal zone of north Queensland.	0.52	-	-	-	-	-	32.88	34.80	15.53	5.41	0.91	0.27	-	-	0.60	0.26	0.39	-	[3]
Canada	INCO's flash smelting furnace, Sudbury, Ontario	0.58	38.6	0.93	-	-	45.40	52.20	17.40	1.11	2.51	1.65	-	-	-	-	-	0.03	0.15	[56, 66]

The analysis of the SEM-EDS image shown in Figure 5 confirms the presence of Fe_2SiO_4 and small traces of Cu in the sample.

The principal minerals and oxides present in the copper slag, including those that represent 1% of the chemical composition, have melting temperatures (*Tm*) very different from each other, which are detailed below: Fe_2SiO_4 (*Tm* = 1216.9 °C) < Cu_2O (*Tm* = 1243.6 °C) < FeO (*Tm* = 1376.9 °C) < Fe_3O_4 (*Tm* = 1596.9 °C) < SiO_2 (*Tm* = 1722.9 °C) < MnO (*Tm* = 1841.9 °C) < ZnO (*Tm* = 1701.9 °C) < Al_2O_3 (*Tm* = 2053.9 °C) < MgO (*Tm* = 2831.9 °C) < CaO (*Tm* = 2926.9 °C) [67]. These temperatures allow us to see that metal oxides could volatilize when exposed to high temperatures and in contact with water steam. Opila et al. [68] indicate that the interaction of high-temperature water steam with oxides to form volatile hydroxides leads to material loss. The following reactions are according to the supposed reaction that could occur during the thermolysis process. The thermal decomposition of Fe_2SiO_4 or 2FeO-SiO_2 mainly involves its transformation into Fe_2O_3, Fe_3O_4, and amorphous silica (SiO_2) [3,64,69]. The oxidation of the slag includes the decomposition of Fe_2SiO_4, and the adsorption and diffusion of superoxide ions (O^{2-}) and other species, promoting the formation of FeO, Fe_2O_3, Fe_3O_4, and SiO_2 [64]. Chen et al. [70] investigated the oxidation behavior of Fe_2SiO_4 in water steam at 1000 °C, reporting that Fe_2SiO_4 was completely decomposed into Fe_3O_4 (58.8 wt%), Fe_2O_3 (21.6 wt%), and SiO_2 (19.6 wt%) (see Equation (5)) and obtained a hydrogen production capacity of 24.42 mL/g. Equation (5) is as follows:

$$3Fe_2SiO_4 + 2H_2O \rightarrow 2Fe_3O_4 + 3SiO_2 + 2H_2 \quad (5)$$

The use of magnetite has been widely investigated, but the production of H_2 from the use of Fe_3O_4 was proposed by Nakamura et al. in 1977 [69,71–76] according to Equation (6), which is as follows:

$$2Fe_3O_4 + H_2O \rightarrow 3Fe_2O_3 + H_2 \quad (6)$$

However, other researchers indicate that when Fe_3O_4 is in contact with water steam it can produce volatile metal oxides (Equation (7)) [77], as can be seen in the following equation:

$$Fe_3O_4 + 2H_2O \rightarrow Fe(OH)_2 + 2FeO(OH) \quad (7)$$

$(Mg_{1-x},Fe_x)_2SiO_4$ [78], which is also written as $2(Mg_{1-x},Fe_x)O–SiO_2$, is a mineral formed between two metals (Fe and Mg) and SiO_2 and is found in a solid solution between Fe_2SiO_4 and Mg_2SiO_4 [79]. Freund et al. [80] proposed that, if H_2O is incorporated into the $(Mg_{1-x},Fe_x)_2SiO_4$ structure, its presence can create extrinsic point defects that are associated with H_2 production due to the formation of OH ions. But the structure of $(Mg_{1-x},Fe_x)_2SiO_4$ has mainly been investigated for the influence it has on the production of H_2 during a serpentinization reaction which is accompanied by volume expansion (serpentine ($Mg_3Si_2O_5(OH)_4$) possibly results from the reaction of water with ferrous minerals rich in Fe that are contained in ultramafic rocks). The generation of H_2 during the serpentinization mechanism is a result of the reaction of water with ferrous iron (Fe^{2+}) derived from minerals, mainly olivine and pyroxene, to ferric iron (Fe^{3+}), which normally precipitates as magnetite. The process was modeled numerically by McCollom et al. [81], indicating that at high temperatures (>315 °C), the rates of serpentinization reactions are fast, and their reaction is represented by Equation (8) which follows:

$$Mg_{1.8}Fe_{0.2}SiO_4 + 1.37H_2O \rightarrow 0.067Fe_3O_4 + 0.5Mg_3Si_2O_5(OH)_4 + 0.3Mg(OH)_2 + 0.067\ H_2 \quad (8)$$

Olsson et al. [82] mention that the dissolution of $(Mg_{1-x},Fe_x)_2SiO_4$ is faster in acidic solutions than in alkaline ones. The acidic solution of $(Mg_{1-x},Fe_x)_2SiO_4$ can be written

as $(Mg,Fe)_2SiO_4 + 4H^+ \geq 2(Mg^{2+},Fe^{2+}) + H_4SiO_4$. As $(Mg_{1-x},Fe_x)_2SiO_4$ dissolves and Si is produced, protons that are consumed cause the pH to increase. Wang et al. [83] also indicate that the dissolution rate of $(Mg_{1-x},Fe_x)_2SiO_4$ is fast relative to other silicates. In the experiments carried out with $(Mg_{1-x},Fe_x)_2SiO_4$ with CO_2/H_2O, they conclude that olivine only reacted with H_2O to produce $Mg_3Si_2O_5(OH)_4$, $(Mg,Fe)(OH)_2$), and Fe_3O_4. The latest research is aimed at estimating the influence of the amount of H_2 on the serpentinization process in a temperature range of 50 to 320 °C through numerical modeling [84]. Silica has been investigated in depth by Opila et al. [68,85,86], who studied the oxidation kinetics of chemically vapor deposited (CVD) silicon carbide (SiC) in the temperature range of 1200–1400 °C [85] and 1000–1400 °C [86] in H_2O/O_2 gas mixtures. They observed that the silica scales formed in SiC can be volatilized simultaneously, forming silicon hydroxide ($SiO(OH)_2$) or silicon oxyhydroxide ($Si(OH)_4$) at atmospheric pressures (0.1 MPa). The formation of volatile hydroxides depends, in some cases, on the partial pressures of water vapor and oxygen, and for processes at 0.1 MPa and temperatures below 1300 °C the volatility of silica can be attributed to the reaction $SiO_2 + 2H_2O \rightarrow Si(OH)_4$. At higher temperatures and at lower partial pressures of water steam and oxygen, the reaction $SiO_2 + H_2O \rightarrow SiO(OH)_2$ is more likely [68]. Kendelewicz et al. [87] studied the adsorption of water on the surface of a single crystal of MnO at low water steam pressures (1.33×10^{-6}–1.33×10^{-2} Pa), in which the reaction with H_2O molecules results in the formation of hydroxyl groups on the surface ($MnO + H_2O \rightarrow Mn(OH)_2$). Another thermodynamic and experimental study of thermochemical cycles (three steps) to produce H_2 involving hydroxides (NaOH and KOH) and MnO among others, has concluded that the reaction of hydroxides with MnO is stable, but they did not produce H_2 at 750 °C, even in strong oxidizing media [88]. Finally, Orfila et al. [89] indicate that the Mn-oxide cycle is the most studied, but unfortunately the H_2O cleavage reactions with MnO are not thermodynamically favorable and the H_2 produced is negligible.

Zn is a metal that when placed in contact with water releases H_2 and produces ZnO. Among the research found, Bilgen et al. [90] carried out the direct decomposition of H_2O in a temperature range of 2000–2500 °C and proposed the exothermic reaction of water vapor, $2Zn + 2H_2O \rightarrow 2ZnO + 2H_2$. Steinfeld [91] considered the production of H_2 from H_2O dissociation through a thermochemical solar cycle (two steps) with ZnO/Zn. In the second step (exothermic, non-solar), they propose the hydrolysis of Zn at 427 °C to form H_2 and ZnO through the reaction $Zn + H_2O \rightarrow ZnO + H_2$. Another study focused on the production of syngas from H_2O and CO_2 in a two-step cycle through Zn/ZnO redox reactions [92]. And recently, Bhosale [93] has proposed a hybrid solar thermochemical cycle of $ZnSO_4$/ZnO for water splitting (WS), with an oxidation step through the reaction $ZnO + SO_2 + H_2O \rightarrow ZnSO_4 + H_2$ at a temperature of 127 °C. Opila et al. [68] indicate that alumina volatilizes in environments containing water steam at high temperatures through the reaction $1/2\ Al_2O_3 + 3/2\ O_2 \rightarrow Al(OH)_3$, but they mention that the volatility of alumina due to the formation of $Al(OH)_3$ is not a problem at temperatures < 1300 °C. Huang et al. [94] indicate that Mg is a good candidate for H_2 generation due to its very low cost, high availability, high theoretical H_2 yield, and the formation of environmentally friendly by-products. The reaction between Mg and H_2O can be described as $Mg + 2H_2O \rightarrow Mg(OH)_2 + H_2$, and this reaction is interrupted due to the formation of a passive layer of $Mg(OH)_2$ on the unreacted Mg particles. Nissen et al. [95] investigated the reaction rate of Ca oxidation with water steam in the temperature range of 25 and 300 °C, obtaining a reaction rate of linear type (at 25 °C) and logarithmic (at 300 °C). In the temperature range of 20–150 °C, Ca reacts according to $Ca + 2H_2O \rightarrow Ca(OH)_2 + H_2$, and at temperatures above 250 °C it reacts according to the mechanism $Ca + H_2O \rightarrow CaO + H_2$. Bhosale [96] thermodynamically analyzed the CaO/Ca-based WS cycle (Ca-WS) using

Metso's chemical reaction and equilibrium software (HSC Chemistry 9.9). Furthermore, they indicate that during the reoxidation of Ca, the result was the formation of H_2.

The oxidation reaction of metal oxides (see Equation (9)), present in copper slag (2FeO-SiO_2, Fe_2O_3, MgO, CaO, MnO, ZnO, K_2O, TiO_2, etc.) [24], can be applied, with the equation as follows:

$$M_xO_y + H_2O \rightarrow M_{x'}O_{y'} + H_2 \quad (9)$$

There is abundant scientific information explaining the interaction between water vapor (H_2O(g)) and Fe under high temperature conditions (200 to 1000 °C), where it is specified that H_2 is produced by the oxidation reaction of Fe and FeO according to Equations (10) and (11) [71,72,97], which are as follows:

$$3Fe + 4H_2O \rightarrow Fe_3O_4 + 4H_2 \quad (10)$$

$$3FeO + H_2O \rightarrow Fe_3O_4 + H_2 \quad (11)$$

On the other hand, the dissociation reaction of water in contact with FeO is favorable at temperatures below 800 °C, when $\Delta G^\circ < 0$ (the reaction is spontaneous and the theoretical conversion of FeO decreases with increasing temperature) [74,98]. Our expectations are that oxides such as Fe_2SiO_4, Fe_3O_4, and $(Mg, Fe)_2SiO_4$ will react with water steam at high temperatures (in a range of 200–1000 °C and 1 atm), generating products such as Fe_3O_4, Fe_2O_3, SiO_2, Mg_2SiO_4, H_2, and possible volatile metal oxides ($M_xO_y(OH)_2$).

The circular economy in mining seeks the recovery, valorization, and reuse of mining waste, transforming it into inputs for new applications instead of disposing of it. According to the above, the use of copper slag in the production of H_2 through thermolysis would represent an important opportunity to transform a waste product that currently plagues the world, especially in desert areas such as the Atacama Desert where mining activity is prevalent, into a high-value-added material, prioritizing its reuse as an alternative application in solar energy. While H_2 production with copper slag is aligned with the principles of the circular economy (see Figure 6), it is essential to assess its environmental impact. The H_2 product of this process can be "reused" as fuel in mining processes, reducing the use of fossil fuels (for example, diesel which is widely used in mining trucks). In addition, by-products such as Fe_3O_4 y Fe_2O_3 can be "recycled" for the recovery of Fe, an element in high demand in Cu smelting.

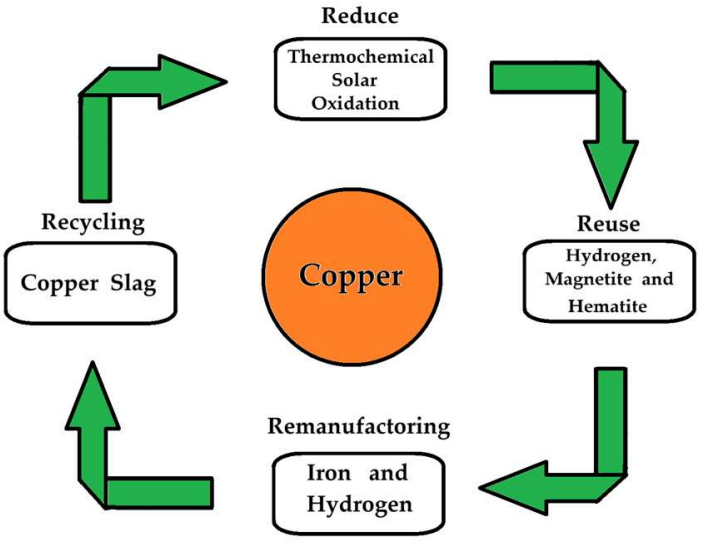


Figure 6. Scheme of the circular economy model applied to copper slag.

The release of heavy metals (Pb, As, and Cd) through volatile metal oxides is unlikely because the thermolysis process must be carried out at temperatures between 200 and 1000 °C, and the majority compound of Chilean copper slag is Fe_2SiO_4 (melting temperature is 1217 °C) and Fe_3O_4 (melting temperature is 1597 °C) [67,99]. To ensure a complete circular economy cycle, the waste generated after thermolysis of copper slag (magnetite and hematite) must be analyzed for possible reuse or Fe recovery, rather than being disposed of, thus maximizing material efficiency. The presence of toxic elements such as As, Cd, and Pb in copper slags depends primarily on the mineralogical composition of the copper concentrate, as well as on the conditions of the smelting process. Complex minerals such as enargite (Cu_3AsS_4) [100–103], tetrahedrite–tennantite ($(Cu,Fe)_{12}(Sb,As)_4S_{13}$) [102,104,105], galena (PbS) [104], and sphalerite (ZnS) [106] containing traces of Cd are the main sources of toxic elements in copper slag. This contamination is the result of flotation processes applied to sulfide ores without strict control over the hydrometallurgical stages. Such operational shortcomings can cause metallic impurities to be carried over into the copper concentrate used in pyrometallurgical processing. In addition, smelters often process blended concentrates from different mining origins, which increases the presence of difficult-to-manage impurities, such as Pb in the form of PbS. During smelting, factors such as temperature, redox atmosphere, and the type of fluxes used influence the final composition of copper slag. Moreover, the recycling of metallurgical dusts or secondary residues can enrich the slag with trace amounts of heavy metals. Therefore, process control and proper stabilization of the slag are essential to minimize the risk of copper slag contamination with toxic materials. At high temperatures (thermolysis process), toxic compounds may pass into the gas phase if not adequately controlled. Currently, copper smelters implement a combination of physical, chemical, and environmental strategies to eliminate or control contaminants such as As and Cd. It is worth noting that Pb is not commonly found as a by-product in copper mining. The removal or control of contaminants in copper smelting is achieved through a combination of physical, chemical, and operational approaches, in which the toxic elements are stabilized as oxides, sulfides, or silicates within glassy or crystalline matrices, reducing their mobility. Simultaneously, at high temperatures during smelting, some of these elements volatilize and are captured by gas treatment systems, producing metallic dusts that require specialized handling. In addition, hydrometallurgical processes are employed to recover or stabilize impurities, such as the removal of As in the form of insoluble compounds like scorodite ($FeAsO_4 \cdot H_2O$) [105] or calcium arsenate ($Ca_3(AsO_4)_2$) [107]. The final disposal of slags and dusts typically involves their stabilization and confinement in controlled storage facilities, with physicochemical encapsulation to prevent leaching. At a preventive level, many smelters also apply source minimization strategies, ensuring the quality control of the concentrate and limiting the input of minerals with high levels of penalized elements.

A major challenge for researchers using copper slag for H_2 production is the potential release of impure gases, such as SO_2, SO_3, and volatile metal species (Pb, As, etc.), during high-temperature reactions. These gases can reduce the purity of the H_2, requiring post-treatment processes before its use in fuel cells or specific industrial applications.

In general, the reduction of Fe_2O_3 does not lead directly to metallic Fe. If the reduction temperature is below 570 °C, the reduction to Fe occurs stepwise from Fe_2O_3 to Fe_3O_4, and continues to Fe. The intermediate oxide, like $Fe_{(1-x)}O$, is not stable at temperatures below 570 °C.

At reduction temperatures above 570 °C, wüstite must also be considered in the reduction process. In this case, the reduction proceeds from Fe_2O_3 through Fe_3O_4 to $Fe_{(1-x)}O$ and then continues to Fe. The following equations show the reduction process at different temperatures [108]:

$$3Fe_2O_3 + H_2 \rightarrow 2Fe_3O_4 + H_2O,\ T < 570\ ^\circ C \quad (12)$$

$$Fe_3O_4 + 4H_2 \rightarrow 3Fe + 4H_2O,\ T > 570\ ^\circ C \quad (13)$$

$$(1 - x)Fe_3O_4 + (1 - 4x)H_2 \rightarrow 3Fe_{(1-x)}O + (1 - 4x)H_2O \quad (14)$$

$$Fe_{(1-x)}O + H_2 \rightarrow (1 - x)Fe + H_2O \quad (15)$$

The presence of sulfur-containing phases such as Cu_2S and FeS_2 would lead to SO_2 emissions, while carbon residues from smelting processes can contribute to CO_2 generation. To mitigate these effects, pretreatment methods or gas scrubbing technologies can be employed to remove impurities after thermolysis. In addition, post-process gas separation techniques, such as selective membranes or pressure swing adsorption (PSA), need to be explored to ensure the high purity of the hydrogen produced.

The efficiency of copper slag in producing H_2 by thermolysis depends on temperature, pressure, and its chemical composition. Studies on iron-based thermochemical cycles have shown that FeO can react with H_2O at temperatures below 1000 °C to generate H_2. However, Fe_2SiO_4 and other silicates in copper slag can reduce the reaction efficiency by stabilizing iron oxides in less reactive forms. To improve the reactivity of copper slag, strategies such as thermal pre-activation (reduction in H_2 or CO atmosphere), the addition of catalytic promoters (Ni, Co), or surface modifications can be explored.

To justify the viability of H_2 production with copper slag, a comparative technical–economic analysis is necessary, evaluating energy efficiency, process scalability, and market demand. In the future, hybrid approaches could be explored, where copper slag is processed in conjunction with other industrial waste to improve overall resource recovery efficiency. However, a substantial advantage is that the copper slag thermolysis process for H_2 production can be integrated with renewable energy, taking advantage of the high solar potential in desert regions such as the Atacama Desert, for example using concentrated solar power (CSP) such as the CSP plant called Cerro Dominador in Chile for high-temperature slag oxidation, medium-temperature concentrated solar power (using parabolic troughs) for steam generation, and photovoltaic energy for electricity consumption. This allows for the design of a completely sustainable system where the slag acts as a reactive material for the production of H_2 without the need for fossil fuels.

This approach allows for closing the resource loop in the mining and energy industries by reusing waste and avoiding dependence on fossil fuels, thereby reducing the carbon footprint of the H_2 production process. Although copper slag is an abundant and inexpensive material, its economic viability in H_2 production must consider the following:

- Costs of collecting and transporting copper slag from smelters to H_2 production plants.
- Pretreatment costs (impurity removal, structural modification).
- Capital expenditures (CAPEXs) and operating costs (OPEXs) for high temperature thermolysis reactors and solar concentrators.
- Costs of purifying water for the process and hydrogen for industrial applications.

A levelized cost of hydrogen (LCOH) analysis should be conducted to assess whether H_2 production using copper slag can compete economically with conventional technologies such as water electrolysis, natural gas reforming (SMR), or biomass gasification. Integration with concentrated solar power (CSP) could significantly improve the process's profitability and sustainability.

Future research is needed to consolidate and scale the use of copper slag as a thermocatalytic material for hydrogen production (and other electrochemical processes), considering approaches from materials science, process engineering, sustainability, and the circular economy. Key areas of focus include the following: (i) advanced thermochemical

and kinetic studies to develop thermodynamic models capable of predicting the energy required for oxidation processes during the interaction between copper slag and water vapor at high temperatures, and to evaluate reaction rates, corrosion behavior, and the specific mechanism of H_2 production during thermolysis; (ii) investigation into the functionalization and modification of copper slag to enhance its catalytic or electrocatalytic activity, for example, through doping with metals such as Ni, Co, or Cu to improve thermal activation under operational conditions; (iii) development and design of electrodes and solar thermolysis reactors to assess solar–thermochemical performance; (iv) environmental and circularity assessments, including life cycle analysis (LCA), with particular emphasis on evaluating the potential of copper slag to substitute exotic materials such as CeO_2.

4. Conclusions

The use of copper slag for hydrogen production via thermolysis represents a compelling and innovative application of circular economy principles to the energy and mining sectors. Globally, more than 30 million tons of copper slag are generated annually, with major producers including Chile, Mexico, Australia, Spain, Namibia, India, and the United States. In northern Chile, particularly in the Atacama Desert, decades of intensive copper smelting have resulted in vast accumulations of copper slag, often stored in large heaps with limited reuse and increasing environmental concern. Although rich in metal oxides such as magnetite and fayalite, copper slag continues to be primarily used in low-value applications such as construction filling and abrasive blasting. Reimagining copper slag as a raw material for hydrogen production marks a significant paradigm shift. Unlike traditional methods such as water electrolysis, which rely on purified water and often require critical and expensive materials (e.g., platinum-based catalysts), the thermolysis of copper slag enables hydrogen generation using a readily available industrial by-product. This approach benefits from several unique advantages, such as the following: (i) extremely low material cost, as copper slag is abundant and often treated as waste; (ii) no requirement for additional reactants, with hydrogen being generated through redox reactions with water vapor; (iii) integration with concentrated solar power (CSP), allowing for carbon-free energy input and significantly lowering operational emissions; (iv) potential for metal recovery (e.g., magnetite, hematite) as a co-benefit, enhancing overall resource efficiency. In regions like the Atacama Desert, where both slag deposits and solar irradiance are abundant, this approach offers a unique opportunity to combine industrial waste recovery with renewable energy to create a local, sustainable pathway for hydrogen production. Moreover, the hydrogen generated through this method could be reintegrated into mining and metallurgical operations, powering microgrids, fueling equipment, or supporting broader decarbonization strategies. This closes material and energy loops, reinforcing circularity in traditionally linear sectors and contributing to the emergence of a low-carbon, green mining economy. Copper slag valorization through solar thermolysis offers a cost-effective, low-emission, and circular alternative to conventional hydrogen production methods. Its success will depend on the continued optimization of reaction conditions, advances in reactor design, and integration with emerging clean technologies. Positioned at the intersection of waste recovery, renewable energy, and green hydrogen, this approach has the potential to contribute meaningfully to national and global clean energy transitions—particularly in resource-rich regions such as the Atacama Desert.

Author Contributions: Conceptualization, M.F., S.L.-G. and F.M.G.M.; methodology, M.F., S.L.-G., V.E.R.C. and F.M.G.M.; validation, A.S. (Alvaro Soliz), F.S., E.F., A.S. (Atul Sagade), M.T. and N.T.; investigation, M.F., N.T., S.L.-G., F.S., J.Á.C.M. and F.M.G.M.; writing—original draft preparation, M.F., S.L.-G. and F.M.G.M.; writing—review and editing, M.F., A.S. (Atul Sagade), F.S., S.L.-G., A.S. (Alvaro Soliz), M.T., N.T. and F.M.G.M.; visualization M.F., A.S. (Alvaro Soliz) and F.M.G.M.; supervision, F.M.G.M. and M.T. All authors have read and agreed to the published version of the manuscript.

Funding: This research received no external funding.

Institutional Review Board Statement: Not applicable.

Informed Consent Statement: Not applicable.

Data Availability Statement: The data presented in this manuscript are available upon request from the corresponding author.

Acknowledgments: The authors would like to thank the Programa de Doctorado en Energía Solar of the Universidad de Antofagasta, Chile. The authors are grateful for the support of ANID-Chile through the research projects FONDECYT Iniciación 11230550 and ANID/FONDAP 1522A0006 Solar Energy Research Center SERC-Chile.

Conflicts of Interest: The authors declare no conflicts of interest.

References

1. Zhang, H.; Hu, C.; Gao, W.; Lu, M. Recovery of Iron from Copper Slag Using Coal-Based Direct Reduction: Reduction Characteristics and Kinetics. *Minerals* **2020**, *10*, 973. [CrossRef]
2. Wang, J.-P.; Erdenebold, U. A Study on Reduction of Copper Smelting Slag by Carbon for Recycling into Metal Values and Cement Raw Material. *Sustainability* **2020**, *12*, 1421. [CrossRef]
3. Gorai, B.; Jana, R.K. Premchand Characteristics and Utilisation of Copper Slag—A Review. *Resour. Conserv. Recycl.* **2003**, *39*, 299–313. [CrossRef]
4. dos Anjos, M.A.G.; Sales, A.T.C.; Andrade, N. Blasted Copper Slag as Fine Aggregate in Portland Cement Concrete. *J. Env. Manag.* **2017**, *196*, 607–613. [CrossRef]
5. Murari, K.; Siddique, R.; Jain, K.K. Use of Waste Copper Slag, a Sustainable Material. *J. Mater. Cycles Waste Manag.* **2015**, *17*, 13–26. [CrossRef]
6. González, C.; Parra, R.; Klenovcanova, A.; Imris, I.; Sánchez, M. Reduction of Chilean Copper Slags: A Case of Waste Management Project. *Scand. J. Metall.* **2005**, *34*, 143–149. [CrossRef]
7. Nazer, A.; Pavez, O.; Rojas, F.; Aguilar, C. *Una Revisión de Los Usos de Las Escorias de Cobre*; Iberomet XI. X Conamet/sam: Viña del Mar, Chile, 2010.
8. Huanosta-Gutiérrez, T.; Dantas, R.F.; Ramírez-Zamora, R.M.; Esplugas, S. Evaluation of Copper Slag to Catalyze Advanced Oxidation Processes for the Removal of Phenol in Water. *J. Hazard. Mater.* **2012**, *213–214*, 325–330. [CrossRef]
9. Shen, H.; Forssberg, E. An Overview of Recovery of Metals from Slags. *Waste Manag.* **2003**, *23*, 933–949. [CrossRef]
10. Wang, X.; Geysen, D.; Padilla Tinoco, S.V.; D'Hoker, N.; Van Gerven, T.; Blanpain, B. Characterisation of Copper Slag in View of Metal Recovery. *Miner. Process. Extr. Metall.* **2015**, *124*, 83–87. [CrossRef]
11. Xue, Y.; Guo, Z.; Zhu, D.; Pan, J.; Wang, Y.; Zhan, R. Efficient Utilization of Copper Slag in an Innovative Sintering Process for Fe–Ni–Cu Alloy Preparation and Valuable Elements Recovery. *J. Mater. Res. Technol.* **2022**, *18*, 3115–3129. [CrossRef]
12. Montoya-Bautista, C.V.; Acevedo-Peña, P.; Zanella, R.; Ramírez-Zamora, R.-M. Characterization and Evaluation of Copper Slag as a Bifunctional Photocatalyst for Alcohols Degradation and Hydrogen Production. *Top. Catal.* **2021**, *64*, 131–141. [CrossRef]
13. Leiva-Guajardo, S.I.; Toro, N.; Fuentealba, E.; Morel, M.J.; Soliz, Á.; Portillo, C.; Galleguillos Madrid, F.M. Contribution of Copper Slag to Water Treatment and Hydrogen Production by Photocatalytic Mechanisms in Aqueous Solutions: A Mini Review. *Materials* **2024**, *17*, 5434. [CrossRef]
14. Segovia, A.V.; Cardemil, J.M.; Sancy, M.; Escobar, R. Analysis of Copper Slag from a Chilean Foundry for Application as Filler Material in Thermal Energy Storage Systems. *J. Energy Storage* **2025**, *111*, 115281. [CrossRef]
15. David-Hernández, M.A.; Calderon-Vásquez, I.; Battisti, F.G.; Cardemil, J.M.; Cazorla-Marín, A. Design and Assessment of a Concentrating Solar Thermal System for Industrial Process Heat with a Copper Slag Packed-Bed Thermal Energy Storage. *Appl. Energy* **2024**, *376*, 124280. [CrossRef]
16. Fernández-González, D.; Prazuch, J.; Ruiz-Bustinza, Í.; González-Gasca, C.; Gómez-Rodríguez, C.; Verdeja, L. Recovery of Copper and Magnetite from Copper Slag Using Concentrated Solar Power (CSP). *Metals* **2021**, *11*, 1032. [CrossRef]

17. Bellan, S.; Kodama, T.; Seok Cho, H.; Kim, J.S. Hydrogen Production by Solar Fluidized Bed Reactor Using Ceria: Euler-Lagrange Modelling of Gas-Solid Flow to Optimize the Internally Circulating Fluidized Bed. *J. Therm. Sci. Technol.* **2022**, *17*, 22–76. [CrossRef]
18. Kodama, T.; Gokon, N.; Cho, H.S.; Bellan, S.; Matsubara, K.; Inoue, K. Particle Fluidized Bed Receiver/Reactor with a Beam-down Solar Concentrating Optics: Performance Test of Two-Step Water Splitting with Ceria Particles Using 30-KWth Sun-Simulator. In Proceedings of the AIP Conference Proceedings; AIP Publishing, M.N.U., Ed.; American Institute of Physics Inc.: College Park, MD, USA, 2018; Volume 2033.
19. Nazer, A.P.; Fuentes, S.; Pavez, O.; Varela, O.; Lanas, O. Baldosas de Escorias de Cobre. Innovación En Producción Limpia. *Iberoam. J. Proj. Manag.* **2012**, *3*, 12.
20. Phiri, T.C.; Singh, P.; Nikoloski, A.N. The Potential for Copper Slag Waste as a Resource for a Circular Economy: A Review–Part I. *Min. Eng.* **2022**, *180*, 107474.
21. Barros, K.S.; Vielmo, V.S.; Moreno, B.G.; Riveros, G.; Cifuentes, G.; Bernardes, A.M. Chemical Composition Data of the Main Stages of Copper Production from Sulfide Minerals in Chile: A Review to Assist Circular Economy Studies. *Minerals* **2022**, *12*, 250. [CrossRef]
22. Pérez, K.; Toro, N.; Gálvez, E.; Robles, P.; Wilson, R.; Navarra, A. Environmental, Economic and Technological Factors Affecting Chilean Copper Smelters—A Critical Review. *J. Mater. Res. Technol.* **2021**, *15*, 213–225. [CrossRef]
23. Alexander, C.; Johto, H.; Lindgren, M.; Pesonen, L.; Roine, A. Comparison of Environmental Performance of Modern Copper Smelting Technologies. *Clean. Environ. Syst.* **2021**, *3*, 100052. [CrossRef]
24. Nazer, A.; Payá, J.; Borrachero, M.V.; Monzó, J. Caracterización de Escorias de Cobre de Fundiciones Chilenas Del Siglo XIX. *Rev. De. Metal.* **2016**, *52*, e083. [CrossRef]
25. Phiri, T.C.; Singh, P.; Nikoloski, A.N. The Potential for Copper Slag Waste as a Resource for a Circular Economy: A Review—Part II. *Min. Eng.* **2021**, *172*, 107150. [CrossRef]
26. Zhou, W.; Liu, X.; Lyu, X.; Gao, W.; Su, H.; Li, C. Extraction and Separation of Copper and Iron from Copper Smelting Slag: A Review. *J. Clean. Prod.* **2022**, 133095. [CrossRef]
27. Zhai, Q.; Liu, R.; Wang, C.; Wen, X.; Li, X.; Sun, W. A Novel Scheme for the Utilization of Cu Slag Flotation Tailings in Preparing Internal Electrolysis Materials to Degrade Printing and Dyeing Wastewater. *J. Hazard. Mater.* **2022**, *424*, 127537. [CrossRef] [PubMed]
28. Guo, Z.; Zhu, D.; Pan, J.; Zhang, F. Innovative Methodology for Comprehensive and Harmless Utilization of Waste Copper Slag via Selective Reduction-Magnetic Separation Process. *J. Clean. Prod.* **2018**, *187*, 910–922. [CrossRef]
29. Kim, B.S.; Jo, S.K.; Shin, D.; Lee, J.C.; Jeong, S.B. A Physico-Chemical Separation Process for Upgrading Iron from Waste Copper Slag. *Int. J. Min. Process* **2013**, *124*, 124–127. [CrossRef]
30. Jin, Q.; Chen, L. A Review of the Influence of Copper Slag on the Properties of Cement-Based Materials. *Materials* **2022**, *15*, 8594. [CrossRef]
31. Rohini, I.; Padmapriya, R. Properties of Bacterial Copper Slag Concrete. *Buildings* **2023**, *13*, 290. [CrossRef]
32. Wu, W.; Zhang, W.; Ma, G. Optimum Content of Copper Slag as a Fine Aggregate in High Strength Concrete. *Mater. Des.* **2010**, *31*, 2878–2883. [CrossRef]
33. Lavanya, C.; Rao, A.S.; Kumar, N.D. Study on Coefficient of Permeability of Copper Slag When Admixed with Lime and Cement. *IOSR J. Mech. Civ. Eng.* **2013**, *7*, 19–25.
34. Salleh, S.; Shaaban, M.G.; Mahmud, H.B.; Kang, J.; Looi, K.T. Production of Bricks from Shipyard Repair and Maintenance Hazardous Waste. *Int. J. Environ. Sci. Dev.* **2014**, *5*, 52. [CrossRef]
35. Arivalagan, S. Experimental Study on the Flexural Behavior of Reinforced Concrete Beams as Replacement of Copper Slag as Fine Aggregate. *J. Civ. Eng. Urban.* **2013**, *3*, 176–182.
36. Ambily, P.S.; Umarani, C.; Ravisankar, K.; Prem, P.R.; Bharatkumar, B.H.; Iyer, N.R. Studies on Ultra High Performance Concrete Incorporating Copper Slag as Fine Aggregate. *Constr. Build. Mater.* **2015**, *77*, 233–240. [CrossRef]
37. Dzinomwa, G.; Mapani, B.; Nghipulile, T.; Maweja, K.; Kurasha, J.T.; Amwaama, M.; Chigayo, K. Mineralogical Characterization of Historic Copper Slag to Guide the Recovery of Valuable Metals: A Namibian Case Study. *Materials* **2023**, *16*, 6126. [CrossRef]
38. Wu, W.; Zhang, W.; Ma, G. Mechanical Properties of Copper Slag Reinforced Concrete under Dynamic Compression. *Constr. Build. Mater.* **2010**, *24*, 910–917. [CrossRef]
39. Brindha, D.; Sureshkumar, P. Buckling Strength of RCC Columns Incorporating Copper Slag as Partial Replacement of Cement. In Proceedings of the National Conference on Emerging Trends in Civil Engineering, Tamil Nadu, India, 23 February 2010.
40. Zhang, Q.; Zhang, B.; Wang, D. Environmental Benefit Assessment of Blended Cement with Modified Granulated Copper Slag. *Materials* **2022**, *15*, 5359. [CrossRef] [PubMed]
41. Sun, L.; Feng, Y.; Wang, D.; Qi, C.; Zeng, X. Influence of CaO on Physical and Environmental Properties of Granulated Copper Slag: Melting Behavior, Grindability and Leaching Behavior. *Int. J. Env. Res. Public Health* **2022**, *19*, 13543. [CrossRef]

42. Pérez, K.; Villegas, Á.; Saldaña, M.; Jeldres, R.I.; González, J.; Toro, N. Initial Investigation into the Leaching of Manganese from Nodules at Room Temperature with the Use of Sulfuric Acid and the Addition of Foundry Slag—Part II. *Sep. Sci. Technol.* **2021**, *56*, 389–394. [CrossRef]
43. Anudeep, R.; Ramesh, K.V.; SowjanyaVani, V. Study on Mechanical Properties of Concrete with Various Slags as Replacement to Fine Aggregate. *Concr. Aggreg. Replace.* **2015**, 86–90.
44. Shi, Y.; Wei, Y.; Zhou, S.; Li, B.; Yang, Y.; Wang, H. Effect of B2O3 Content on the Viscosity of Copper Slag. *J. Alloys Compd.* **2020**, *822*, 153478. [CrossRef]
45. Lewowicki, S.; Rajczyk, J. The Usefulness of Copper Metallurgical Slag as a Micro-Aggregate Additive in Mortars and Concrete Mixtures. In Proceedings of the 13 International Conference on Solid Waste Technology and Management, Philadelphia, PA, USA, 16 November 1997; Volume 2.
46. Alanoca, S. El Mercado Mundial de Fundiciones de Cobre. Situación, Cambios y Desafíos Para Chile. Available online: https://d1wqtxts1xzle7.cloudfront.net/111040568/El_mercado_mundial_de_fundiciones_de_Cobre._Situacion_cambios_y_desafios_para_Chile._SA_46_pag._09.2022_-libre.pdf (accessed on 11 January 2025).
47. Chun, T.; Ning, C.; Long, H.; Li, J.; Yang, J. Mineralogical Characterization of Copper Slag from Tongling Nonferrous Metals Group China. *JOM* **2016**, *68*, 2332–2340. [CrossRef]
48. Ma, Q.; Du, H.; Zhou, X.; He, K.; Lin, Z.; Yan, F.; Huang, L.; Guo, R. Performance of Copper Slag Contained Mortars after Exposure to Elevated Temperatures. *Constr. Build. Mater.* **2018**, *172*, 378–386. [CrossRef]
49. Fuentes, M.; Pulido, D.; Fuentealba, E.; Soliz, A.; Toro, N.; Sagade, A.; Galleguillos Madrid, F.M. Direct Solar Thermal Water-Splitting Using Iron and Iron Oxides at High Temperatures: A Review. *Appl. Sci.* **2024**, *14*, 7056. [CrossRef]
50. Li, P.; Chen, Y.; Li, X.; Yan, B.; Chen, D.; Guo, H. Hydrogen Generation Characteristics of Steel Slag-Steam High Temperature Reaction in Terms of Particle Size. *Int. J. Hydrogen Energy* **2020**, *45*, 17140–17152. [CrossRef]
51. Li, P.; Guo, H.; Gao, J.; Min, J.; Yan, B.; Chen, D.; Seetharaman, S. Novel Concept of Steam Modification towards Energy and Iron Recovery from Steel Slag: Oxidation Mechanism and Process Evaluation. *J. Clean. Prod.* **2020**, *254*, 119952. [CrossRef]
52. Perez, N. *Electrochemistry and Corrosion Science*; Perez, N., Ed.; Kluwer Academic Publishers: New York, NY, USA, 2004; ISBN 1-4020-7744-0.
53. Etievant, C. Solar Energy Materials Solar High-Temperature Direct Water Splitting a Review of Experiments in France. *Sol. Energy Mater.* **1991**, *24*, 413–440. [CrossRef]
54. Meredig, B.; Wolverton, C. First-Principles Thermodynamic Framework for the Evaluation of Thermochemical H_2O- Or CO_2-Splitting Materials. *Phys. Rev. B Condens. Matter Mater. Phys.* **2009**, *80*, 245119. [CrossRef]
55. Johansen, E.-B.; Rosenqvist, T.; Torgersen, P.T. On the Thermodynamics of Continuous Copper Smelting. *JOM* **1970**, *22*, 39–47. [CrossRef]
56. Tian, H.; Guo, Z.; Pan, J.; Zhu, D.; Yang, C.; Xue, Y.; Li, S.; Wang, D. Comprehensive Review on Metallurgical Recycling and Cleaning of Copper Slag. *Resour. Conserv. Recycl.* **2021**, *168*, 105366. [CrossRef]
57. Saez, R.; Nocete, F.; Nieto, J.M.; Capitan, M.A.; Rovira, S. The Extractive Metallurgy of Copper from Cabezo Jure, Huelva, Spain: Chemical and Mineralogical Study of Slags Dated to the Third Millenium b.c. *Can. Mineral.* **2003**, *41*, 627–638. [CrossRef]
58. Salmerón, C.; Fernando, O.; García, C.; De Lourdes, M.; Mejía, G.; Ariadna, T. Estudio Preliminar de Escoria de Cobre Como Precursor Potencial Para La Síntesis de Geopolímeros 2015. Available online: https://zaloamati.azc.uam.mx/bitstreams/6a85c67a-8689-42ea-9f2e-24cb164521fa/download (accessed on 10 January 2025).
59. Pérez Segura, E.; Coronado López, H.; Robles Vega, A.; Brown Bojórquez, F. Mineralogía y Posibilidades de Recuperación de Cobre de La Escoria de La Planta Fundidora Del Complejo Minero-Metalúrgico de La Caridad, Sonora. *RIIIT. Rev. Int. Investig. E Innovación Tecnológica* **2016**, *4*, 1–20.
60. Gómez-Rodríguez, C.; Antonio-Zárate, Y.; Revuelta-Acosta, J.; Verdeja, L.F.; Fernández-González, D.; López-Perales, J.F.; Rodríguez-Castellanos, E.A.; García-Quiñonez, L.V.; Castillo-Rodríguez, G.A. Research and Development of Novel Refractory of MgO Doped with ZrO_2 Nanoparticles for Copper Slag Resistance. *Materials* **2021**, *14*, 2277. [CrossRef]
61. Manasse, A.; Mellini, M.; Viti, C. The Copper Slags of the Capattoli Valley, Campiglia Marittima, Italy. *Eur. J. Mineral.* **2001**, *13*, 949–960. [CrossRef]
62. Sánchez, M.; Sudbury, M. Physicochemical Characterization of Copper Slag and Alternatives of Friendly Environmental Management. *J. Min. Metall. Sect. B Metall.* **2013**, *49*, 161–168. [CrossRef]
63. Mateus, A.; Pinto, A.; Alves, L.C.; Matos, J.X.; Figueiras, J.; Neng, N.R. Roman and Modern Slag at S. Domingos Mine (IPB, Portugal): Compositional Features and Implications for Their Long-Term Stability and Potential Reuse. *Int. J. Env. Waste Manag.* **2011**, *8*, 133. [CrossRef]
64. Gyurov, S.; Rabadjieva, D.; Kovacheva, D.; Kostova, Y. Kinetics of Copper Slag Oxidation under Nonisothermal Conditions. *J. Therm. Anal. Calorim.* **2014**, *116*, 945–953. [CrossRef]
65. Lohmeier, S.; Lottermoser, B.G.; Schirmer, T.; Gallhofer, D. Copper Slag as a Potential Source of Critical Elements—A Case Study from Tsumeb, Namibia. *J. S. Afr. Inst. Min. Met.* **2021**, *121*, 129–142. [CrossRef]

66. Gbor, P.K.; Mokri, V.; Jia, C.Q. Characterization of Smelter Slags. *J. Environ. Sci. Health Part. A* **2000**, *35*, 147–167. [CrossRef]
67. Barin, I.; Platzhi, G. *Thermochemical Data of Pure Substances*; Wiley: Wienheim, Germany, 1989; Volume 304, ISBN 3527287450.
68. Opila, E.J.; Jacobson, N.S.; Myers, D.L.; Copland, E.H. Predicting Oxide Stability in High-Temperature Water Vapor. *JOM* **2006**, *58*, 22–28. [CrossRef]
69. Li, X.; Ma, Y.; Xing, X. Recovery of Iron from Nickel Slag in Water Vapor at High Temperature. *JOM* **2023**, *75*, 331–339. [CrossRef]
70. Chen, J.H.; Mi, W.J.; Chen, H.Y.; Li, B.; Chou, K.C.; Hou, X.M. Iron Oxide Recovery from Fayalite in Water Vapor at High Temperature. *J. Min. Metall. Sect. B Metall.* **2018**, *54*, 1–8. [CrossRef]
71. Nakamura, T. Hydrogen Production from Water Utilizing Solar Heat at High Temperatures. *Sol. Energy* **1977**, *19*, 467–475. [CrossRef]
72. Steinfeld, A.; Sanders, S.; Palumbo, R. Design Aspects of Solar Thermochemical Engineering-a Case Study: Two-Step Water-Splitting Cycle Using the Fe_3O_4/FeO Redox System. *Solar Energy* **1999**, *65*, 43–53. [CrossRef]
73. Kodama, T. High-Temperature Solar Chemistry for Converting Solar Heat to Chemical Fuels. *Prog. Energy Combust. Sci.* **2003**, *29*, 567–597.
74. Kodama, T.; Gokon, N. Thermochemical Cycles for High-Temperature Solar Hydrogen Production. *Chem. Rev.* **2007**, *107*, 4048–4077. [PubMed]
75. Palumbo, R.; Diver, R.B.; Larson, C.; Coker, E.N.; Miller, J.E.; Guertin, J.; Schoer, J.; Meyer, M.; Siegel, N.P. Solar Thermal Decoupled Water Electrolysis Process I: Proof of Concept. *Chem. Eng. Sci.* **2012**, *84*, 372–380. [CrossRef]
76. Young, D.J.; Watson, S. High-Temperature Corrosion in Mixed Gas Environments. *Oxid. Met.* **1995**, *44*, 239–264. [CrossRef]
77. Svoboda, K.; Slowinski, G.; Rogut, J.; Baxter, D. Thermodynamic Possibilities and Constraints for Pure Hydrogen Production by Iron Based Chemical Looping Process at Lower Temperatures. *Energy Convers. Manag.* **2007**, *48*, 3063–3073. [CrossRef]
78. Michel, R.; Ammar, M.R.; Véron, E.; Simon, P.; Poirier, J. Investigating the Mechanism of Phase Transformations and Migration in Olivine at High Temperature. *RSC Adv.* **2014**, *4*, 26645–26652. [CrossRef]
79. van Genuchten, C.M.; Hamaekers, H.; Fraiquin, D.; Hollanders, S.; Ahmad, A. Heavy Metal Removal Potential of Olivine. *Water Res.* **2023**, *245*, 120583. [CrossRef] [PubMed]
80. Freund, F.; Oberheuser, G. Water Dissolved in Olivine: A Single-crystal Infrared Study. *J. Geophys. Res. Solid Earth* **1986**, *91*, 745–761.
81. McCollom, T.M.; Bach, W. Thermodynamic Constraints on Hydrogen Generation during Serpentinization of Ultramafic Rocks. *Geochim. Cosmochim. Acta* **2009**, *73*, 856–875. [CrossRef]
82. Olsson, J.; Bovet, N.; Makovicky, E.; Bechgaard, K.; Balogh, Z.; Stipp, S.L.S. Olivine Reactivity with CO_2 and H_2O on a Microscale: Implications for Carbon Sequestration. *Geochim. Cosmochim. Acta* **2012**, *77*, 86–97. [CrossRef]
83. Wang, J.; Watanabe, N.; Okamoto, A.; Nakamura, K.; Komai, T. Acceleration of Hydrogen Production during Water-Olivine-CO_2 Reactions via High-Temperature-Facilitated Fe(II) Release. *Int. J. Hydrogen Energy* **2019**, *44*, 11514–11524. [CrossRef]
84. Shestopalov, V.M.; Koliabina, I.L.; Ponomarenko, O.M.; Lukin, A.Y.; Rud, A.D. Thermodynamic Assessment of the Possibility of Olivine Interaction with Deep-Seated Hydrogen. *Int. J. Hydrogen Energy* **2022**, *47*, 7062–7071. [CrossRef]
85. Opila, E.J.; Hann Jr, R.E. Paralinear Oxidation of CVD SiC in Water Vapor. *J. Am. Ceram. Soc.* **1997**, *80*, 197–205.
86. Opila, E.J. Variation of the Oxidation Rate of Silicon Carbide with Water-vapor Pressure. *J. Am. Ceram. Soc.* **1999**, *82*, 625–636.
87. Kendelewicz, T.; Doyle, C.S.; Carrier, X.; Brown Jr, G.E. Reaction of Water with Clean Surfaces of MnO (100). *Surf. Rev. Lett.* **1999**, *6*, 1255–1263.
88. Charvin, P.; Abanades, S.; Lemort, F.; Flamant, G. Hydrogen Production by Three-Step Solar Thermochemical Cycles Using Hydroxides and Metal Oxide Systems. *Energy Fuels* **2007**, *21*, 2919–2928.
89. Orfila, M.; Linares, M.; Molina, R.; Botas, J.Á.; Marugán, J.; Sanz, R. Thermochemical Hydrogen Production Using Manganese Cobalt Spinels as Redox Materials. *Int. J. Hydrogen Energy* **2017**, *42*, 13532–13543. [CrossRef]
90. Bilgen, E.; Ducarroir, M.; Foex, M.; Sibieude, F.; Trombe, F. Use of Solar Energy for Direct and Two-Step Water Decomposition Cycles. *Int. J. Hydrogen Energy* **1977**, *2*, 251–257. [CrossRef]
91. Steinfeld, A. Solar Hydrogen Production via a Two-Step Water-Splitting Thermochemical Cycle Based on Zn/ZnO Redox Reactions. *Int. J. Hydrogen Energy* **2002**, *27*, 611–619. [CrossRef]
92. Loutzenhiser, P.G.; Steinfeld, A. Solar Syngas Production from CO_2 and H_2O in a Two-Step Thermochemical Cycle via Zn/ZnO Redox Reactions: Thermodynamic Cycle Analysis. *Int. J. Hydrogen Energy* **2011**, *36*, 12141–12147. [CrossRef]
93. Bhosale, R.R. H2 Producing Hybrid Solar Thermochemical ZnSO4/ZnO Water Splitting Cycle: Thermodynamic Efficiency Analysis. *Int. J. Hydrogen Energy* **2024**, *49*, 1584–1592. [CrossRef]
94. Huang, M.; Ouyang, L.; Chen, Z.; Peng, C.; Zhu, X.; Zhu, M. Hydrogen Production via Hydrolysis of Mg-Oxide Composites. *Int. J. Hydrogen Energy* **2017**, *42*, 22305–22311. [CrossRef]
95. Nissen, D.A. The Low-Temperature Oxidation of Calcium by Water Vapor. *Oxid. Met.* **1977**, *11*, 241–261. [CrossRef]
96. Bhosale, R.R. H2 Generation via Solar Assisted CaO/Ca Thermochemical H_2O Splitting Cycle. *Int. J. Hydrogen Energy* **2021**, *46*, 12095–12104. [CrossRef]

97. Whitney, W.R. The Corrosion of Iron. *J. Am. Chem. Soc.* **1903**, *25*, 394–406. [CrossRef]
98. Abanades, S. Metal Oxides Applied to Thermochemical Water-Splitting for Hydrogen Production Using Concentrated Solar Energy. *ChemEngineering* **2019**, *3*, 63. [CrossRef]
99. Robie, R.A.; Hemingway, B.S. *Thermodynamic Properties of Minerals and Related Substances at 298.15 K. and 1 Bar. (105 Pascals) Pressure and at Higher Temperatures (No. 2131)*; U.S. G.P.O.: Washington, DC, USA, 1995.
100. Lattanzi, P.; Da Pelo, S.; Musu, E.; Atzei, D.; Elsener, B.; Fantauzzi, M.; Rossi, A. Enargite Oxidation: A Review. *Earth Sci. Rev.* **2008**, *86*, 62–88. [CrossRef]
101. Conner, K.; Anderson, C. Enargite Treatments and Pressure Oxidation of Concentrates. *J. Metall. Eng.* **2013**, *2*, 115–123.
102. Zhou, S.; Li, T.; Wang, C.; Tan, Z.; Guan, X.; Li, H.; Zhang, W. Tennantite and Enargite Rejection in the Copper Flotation—A Mini-Review. *J. Miner. Mater. Charact. Eng.* **2023**, *11*, 63–68. [CrossRef]
103. Véliz, M.; Aracena, A.; Jerez, O.; Pérez-Tello, M.; Balladares, E. Copper Sulfation from Enargite Roasting Using Coal and Fayalite Slag Mixture. *Minerals* **2023**, *13*, 1489. [CrossRef]
104. Baken, S.; Delbeke, K.; Rodriguez, P.H. Copper Concentrates: Environmental and Human. Health Hazard. Classification. 2023. Available online: https://internationalcopper.org/wp-content/uploads/2024/02/ICA-Copper-con-classification-guidance-1.pdf (accessed on 13 January 2025).
105. Charitos, A.; Wrobel, M.; Runkel, M.; Hammerschmidt, J.; Demopoulos, G.P. Partial Roasting Combined with Scorodite Technology for Efficient Arsenic Removal and Stabilization from Cu-Concentrates. In Proceedings of the Conference of Metallurgists, Halifax, NS, Canada, 19 August 2024; Springer: Berlin, Germany, 2024; pp. 327–335.
106. Manca, P.P.; Massacci, G.; Pintus, D.; Sogos, G. The Flotation of Sphalerite Mine Tailings as a Remediation Method. *Min. Eng.* **2021**, *165*, 106862. [CrossRef]
107. Liang, Q.; Jiang, L.; Zheng, J.; Duan, N. Mechanism Study of the Effect of Copper Ions on the Stability of As(III) Sulfuration Precipitation in Acidic Copper Smelting Wastewater. *Env. Monit. Assess.* **2024**, *197*, 36. [CrossRef]
108. Spreitzer, D.; Schenk, J. Reduction of Iron Oxides with Hydrogen—A Review. *Steel Res. Int.* **2019**, *90*, 1900108. [CrossRef]

Disclaimer/Publisher's Note: The statements, opinions and data contained in all publications are solely those of the individual author(s) and contributor(s) and not of MDPI and/or the editor(s). MDPI and/or the editor(s) disclaim responsibility for any injury to people or property resulting from any ideas, methods, instructions or products referred to in the content.